

Ultrastretchable and Stable Conductive Elastomer Based on Micro-Ionicgel for Wide-Working-Range Sensors

Xiaohui Yu, Yufei Wang, Haopeng Zhang, Xiaoshan Fan,* and Tianxi Liu*

Cite This: *ACS Appl. Mater. Interfaces* 2021, 13, 53091–53098

Read Online

ACCESS |



Metrics & More



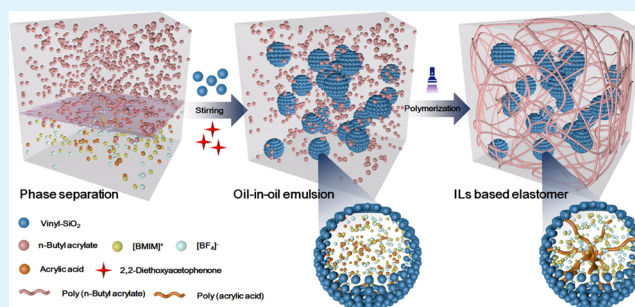
Article Recommendations



Supporting Information

ABSTRACT: A facile route to novel stretchable conductive elastomers with micro-ionicgel acting as conductive fillers was developed via oil-in-oil Pickering emulsion polymerization of nonpolar monomers A and a mixture of polar monomers B and ionic liquids (ILs). Oil-in-oil Pickering emulsions were first fabricated by mixing *n*-butyl acrylate (*n*-BA), acrylic acid (AA), ionic liquid (1-butyl-3-methylimidazolium tetrafluoroborate, [EMIM]⁺[BF₄]⁻), and alkyl vinyl-functionalized silica particles. The emulsion structure was directly observed using the dye-labeled AA-IL phase by confocal fluorescence microscopy. Upon polymerization, the IL-based conductive composite elastomers were obtained, where the continuous phase and the dispersed phase are poly(*n*-butyl acrylate) (PnBA) and poly(acrylic acid) containing ILs (PAA-ILs, referred to as micro-ionicgel), respectively. The PnBA matrix endows the formed elastomer with extremely large stretchability (up to 12 000% strain) and insensitivity to moisture. The micro-ionicgels PAA-ILs not only contribute to good conductivity but can also prevent the leakage of ILs upon stretching or folding. The electrical impedance-based stretchable sensors fabricated using this IL elastomer could detect various human motions including the bending of a finger, wrist, elbow, and knee. Therefore, the as-developed sensors show promising applications for human–machine interfaces of flexible wearable sensors.

KEYWORDS: ionic liquids, Pickering emulsion, conductive elastomer, ultrastretchable, wearable sensor



1. INTRODUCTION

Flexible pressure and strain wearable sensors, which are capable of transducing mechanical deformations into electrical signals, have shown significant promise for a broad range of applications such as human–machine interfaces,^{1–3} personal healthcare diagnosis,⁴ and activity monitoring.⁵ Both flexible pressure and strain sensors require conductive elastomers serving as stretchable electrodes in capacitive or resistive circuit elements.^{6,7} Currently, the reported conductive elastomers are mostly fabricated by incorporating conductive fillers (carbon materials,^{8–10} conducting polymers,^{11,12} and metal nanowires^{13,14}) into the flexible polymer matrix to form a conductive network.¹⁵ Although the sensors fabricated using these elastomers could monitor small strains or pressure with high sensitivity, they display limited stretchability (less than 200%) due to the large difference between Young's moduli of the soft matrix and the rigid filler.^{16–18} Meanwhile, these sensors usually suffer from rapid deterioration in conductivity because of the separation and breakage of the integrated conductive fillers under repeated large deformation, thereby significantly limiting their applications.¹⁹ Another route toward preparation of conductive elastomers is to coat the conductive layers onto the surface of elastomeric substrates such as poly(dimethylsiloxane).²⁰ Even though the obtained sensors exhibit good stretchable properties, the conductive layers are

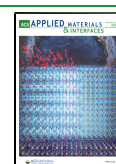
easily delaminated or peel off from the substrate upon stretching, bending, or scratching, resulting in deterioration or even failure of the electrical performance.^{21,22} In addition, this strategy suffers from the complexity and high cost of the manufacturing processes. Therefore, extremely stretchable conductive elastomers with antifatigue conductivity are of significance to developing high-performance flexible wearable sensors.

Ionic liquids (ILs) have unique characteristics such as high conductivity, high thermal and chemical stability, low viscosity, and nonflammability.^{23,24} Due to this reason, IL-based conductive elastomers have started to receive increasing attention from researchers for the development of novel improved sensors.^{13,25–27} Ionic liquid conductive elastomers are usually fabricated by incorporating the ionic liquid into a flexible matrix, achieving conductivity by ionic transportation through polymer chains.⁷ In particular, ionic liquid conductive elastomers show good stretchability,²⁸ high conductivity,^{29,30}

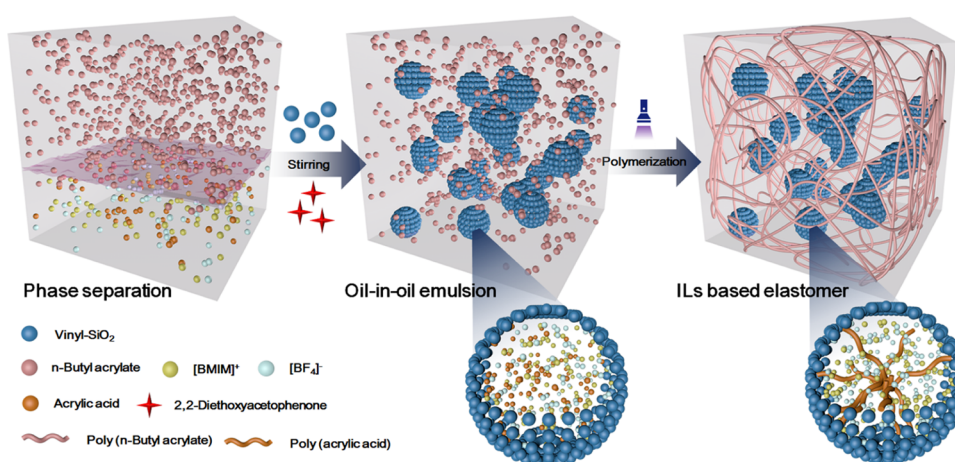
Received: August 23, 2021

Accepted: October 19, 2021

Published: October 27, 2021



Scheme 1. Schematic Illustration of the IL-Based Conductive Elastomer Formed via Oil-in-oil Pickering Emulsion Polymerization



and a wide range operating temperatures,³¹ which are extremely difficult or even impossible to realize by traditional conductive composite elastomers. IL conductive elastomers, however, often suffer from some limitations inherent to ILs. Due to the high hydrophilicity of ILs, IL conductive elastomers are usually unstable in ambient conditions, which could cause an alteration of various properties including stretchability and conductivity.³² Meanwhile, IL elastomers confront the problem of leakage when subjected to external mechanical forces (including stretching and folding).^{33,34} Furthermore, most elastomers with good stretchability are nonpolar and hydrophobic; thus, the fabrication of IL-based elastomers is largely restricted to the miscibility of many elastomers with ILs.^{35,36} Thus far, reports on IL elastomers with large stretchability and high stability are rare, and newly designed strategies enabling high-performance IL elastomers are desirable.

Herein, we reported a versatile and simple strategy for the fabrication of high-performance IL-based conductive elastomers via oil-in-oil Pickering emulsion polymerization (Scheme 1). Specifically, the emulsion consists of the nonpolar continuous phase of *n*-BA monomers and the polar dispersed phase of a mixture of AA monomers and ILs, using alkyl vinyl-functionalized silica particles as the surfactant. Upon ultraviolet light irradiation, the *n*-BA phase polymerized to form the elastic matrix, while the mixture of AA and ILs formed the micro-ionicgel PAA-ILs. Thus, conductive elastomers possessing the sea-island unique architecture were obtained. The PnBA matrix contributes to the extremely high stretchability (up to 12 000%) of the resulting materials, rendering them one of the most stretchable IL-based elastomers reported so far. In addition, PAA-IL micro-ionicgels acting as novel conductive fillers endows them with good conductivity and a wide range of operating temperatures. Importantly, the resulting IL-based conductive elastomers can avoid the instability caused by moisture absorption from the air and the IL leakage during deformation. To demonstrate the applications of the prepared IL-based elastomers, electrical impedance-based stretchable sensors were constructed that can sensitively detect different human motions. With such advantages, the prepared IL-based elastomers are expected to be widely used as ideal sensors for flexible electronic devices.

2. EXPERIMENTAL METHODS

2.1. Materials. Acrylic acid (AA) and *n*-butyl acrylate (*n*-BA) were obtained from Sigma-Aldrich Co. The ionic liquid (1-butyl-3-methylimidazolium tetrafluoroborate, [EMIM]⁺[BF₄]⁻) was purchased from TCI Co. Nanosilica white powders (average diameter was 30 nm), 3-aminopropyl trimethoxysilane, triethylamine, 2,2-diethoxyacetophenone, ϵ -caprolactone, and methacryloyl chloride were purchased from Shanghai Aladdin Co. Toluene, tetrahydrofuran, and triethylamine were obtained from Macklin Co. All of the solvents were dried using a solvent purification system. VHB tape was purchased from Minnesota Mining and Manufacturing (3M) Co.

2.2. Characterization. Microscope photography was carried out on an Olympus BX-53M instrument, and the photographs were analyzed using ImageJ. Fourier transform infrared (FT-IR) spectra were obtained using a Nicolet 670 spectrometer with the attenuated total reflectance (ATR) accessory. Thermal gravimetric analysis (TGA) was performed on a TG 209 F1 from room temperature to 500 °C in a N₂ atmosphere with a heating rate of 10 °C min⁻¹. Scanning electron microscopy (SEM) observation was performed with a JSM-7500F (JEOL, Japan) at an operation voltage of 5 kV. The conductivity of IL-CE₈₀ was measured by the four-point probe resistivity test using the 4-Point probe resistivity measurement system (RTS-8) with a size of 1 × 5 × 5 mm³. The ¹H nuclear magnetic resonance (¹H NMR) spectrum of IL-CE was recorded on an AVANCE III 600 MHz NMR spectrometer using CDCl₃ as the solvent. Gel permeation chromatographic (GPC) analysis was conducted using the 1260 Infinity II system, equipped with two Phenomenex linear 5 mm Styragel columns, and THF was used as an eluent at a flow rate of 1.0 mL min⁻¹.

2.3. Preparation of Vinyl-SiO₂. The synthesis of vinyl-SiO₂ was carried out according to a method previously reported by us.³⁷ First, 3.5 g of silica particles and 5 mL of 3-aminopropyl trimethoxysilane were added into a 250 mL flask, followed by the addition of toluene (200 mL) to form a uniform solution. After constant stirring for 12 h at 90 °C, the amino group-modified silica (SiO₂-NH₂) was obtained. Next, 1.2 g of SiO₂-NH₂ and 7.5 g of ϵ -caprolactone were dissolved in 200 mL of tetrahydrofuran. Hydroxyl hybrid silica (SiO₂-R-OH) was obtained after stirring for 12 h at room temperature. Finally, 1.3 g of SiO₂-R-OH, 0.5 mL of methylacryloyl chloride, and 0.45 mL of triethylamine were added to 100 mL of tetrahydrofuran under vigorous stirring for 12 h at room temperature, and vinyl-SiO₂ was obtained. All of the modified silica was collected by centrifugation and stored at 2–8 °C in a nitrogen atmosphere.

2.4. Preparation of the Ionic Liquid Composite Conductive Elastomer. The vinyl hybrid silica could play the role of surfactant to form the Pickering emulsion. First, 0.6 mL of *n*-BA, 0.1 mL of AA, 0.25 mL of 1-butyl-3-methylimidazolium tetrafluoroborate, and 10 mg of 2, 2-diethoxyacetophenone were mixed under violent stirring. With

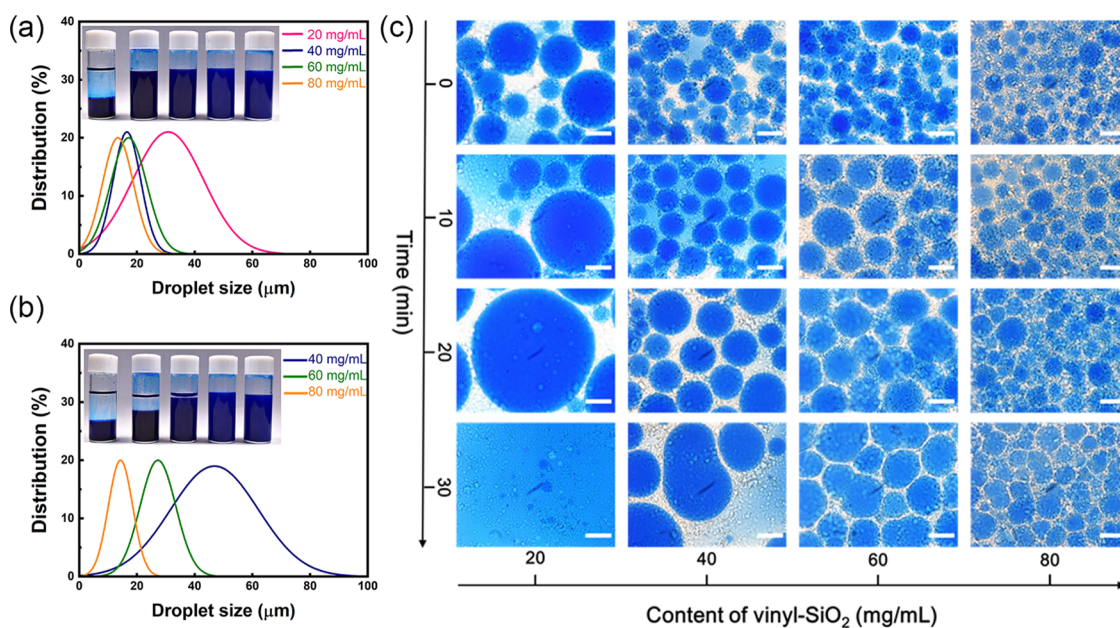


Figure 1. Diameter distribution of droplets in (a) 0 min and (b) 30 min with different vinyl-SiO₂ concentrations. (c) Optical micrographs of Pickering emulsions prepared with varying concentrations of vinyl hybrid silica, 20, 40, 60, and 80 mg/mL, in 30 min (the scale bar is 10 μm).

the introduction of vinyl hybrid silica, a homogeneous solution was obtained. The precursor solution was transferred to a PTFE mold (30 × 10 × 1 mm³) and polymerized under UV light for 2 h ($\lambda = 365$ nm, power = 8 W). The ionic liquid composite conductive elastomer was denoted as IL-CE _{χ} , where χ represents the content of vinyl-SiO₂. Namely, IL-CE₄₀, IL-CE₆₀, and IL-CE₈₀ indicate that the content was 40, 60, and 80 mg/mL, respectively.

3. RESULTS AND DISCUSSION

The fabrication procedure of IL-based conductive elastomer PnBA/SiO₂/PAA-ILs via oil-in-oil Pickering emulsion is described in Scheme 1, which includes two steps. First, *n*-BA, AA, ILs, vinyl-SiO₂, and a photoinitiator were mixed together to form a relatively stable emulsion. Second, the resulting emulsion was polymerized by being subjected to ultraviolet light irradiation (365 nm) to produce the elastomers (denoted as IL-CE _{χ} , where χ is the content of vinyl-SiO₂ in the feed (20, 40, 60, and 80 mg/mL). The deliberate design using micro-ionicgel as conductive fillers was the critical point of this system, which could dissolve two key issues for applications of IL-based conductive elastomers, namely, (i) instability caused by absorbing moisture from the air and (ii) leakage of ILs upon stretching and folding.

First, hydrophobic silica nanoparticles tailored with alkyl chains as the surfactant were prepared according to the process shown in Scheme S1.³⁷ Active amino groups were first introduced onto the surface of bare SiO₂ particles to produce SiO₂-NH₂. Subsequently, the as-prepared SiO₂-NH₂ reacted with ϵ -caprolactone to afford the hydroxyl hexyl-functionalized silica particles SiO₂-R-OH (R:CO(CH₂)₅-OH). Finally, the as-prepared SiO₂-R-OH further reacted with methacryloyl chloride to give the particle surfactant vinyl-SiO₂. It should be pointed out that the alkyl chains grafted onto the SiO₂ surface are necessary for the formation of stable emulsion, while the end vinyl groups play the role of cross-linkers for enhancing the interface interactions of two immiscible phases as the emulsion is cured. Functionalization of SiO₂ was verified by FT-IR and TGA characterizations. As shown in Figure S1c, the peaks observed at 1670 and 940 cm⁻¹ originated from the

characteristic stretching of the vinyl groups, which demonstrated the successful tethering of vinyl alkyl chains onto the surface of SiO₂.^{38,39} Figure S2 shows the TGA analysis of SiO₂-NH₂, SiO₂-R-OH, and vinyl-SiO₂. In comparison with SiO₂-NH₂, the samples of SiO₂-R-OH and vinyl-SiO₂ exhibited increasing weight loss (8 and 36%, respectively), further informing the successful tethering of vinyl alkyl chains onto the surface of SiO₂.³⁹

Due to the successful vinyl alkyl chain grafting, the obtained vinyl-SiO₂ particles were utilized as good solid particle emulsifiers to prepare the Pickering emulsion. The effect of the concentration of vinyl-SiO₂ on the stability of the formed Pickering emulsion was investigated by varying vinyl-SiO₂ concentrations. Figure 1a,b shows the optical pictures of Pickering emulsion with varied concentrations of vinyl-SiO₂ at 20, 40, 60, and 80 mg/mL at 0 min and 30 min. It can be seen that the Pickering emulsion displayed obviously layered phase separation with the addition of 20 mg/mL vinyl-SiO₂ and the color difference of the whole system gradually disappeared with the concentration of vinyl-SiO₂ increasing, indicating the formation of more uniform Pickering emulsion. It is well known that an increasing amount of the added solid particle emulsifiers adsorbing at the biphasic interface results in the increasing contact area of the phase interface, implying the formation of a more stable emulsion. After 30 min, obvious phase separation occurred in the systems with lower emulsifier concentrations (20 and 40 mg/mL), further confirming that the stability of the Pickering emulsion largely depended on the content of vinyl-SiO₂. The prepared Pickering emulsions with different concentrations of vinyl-SiO₂ were further observed using the dye-labeled AA-IL phase by confocal fluorescence microscopy, and Figure 1c shows their polarized micrographs. When the concentration of vinyl-SiO₂ was 20 mg/mL, polydispersed AA-IL droplets with an average size of about 35 μm were first produced, but we failed to obtain stable emulsion as the droplets gradually coalesced into larger ones during 30 min, indicating the insufficiency of the particle emulsifiers. As for the emulsions with the concentrations of

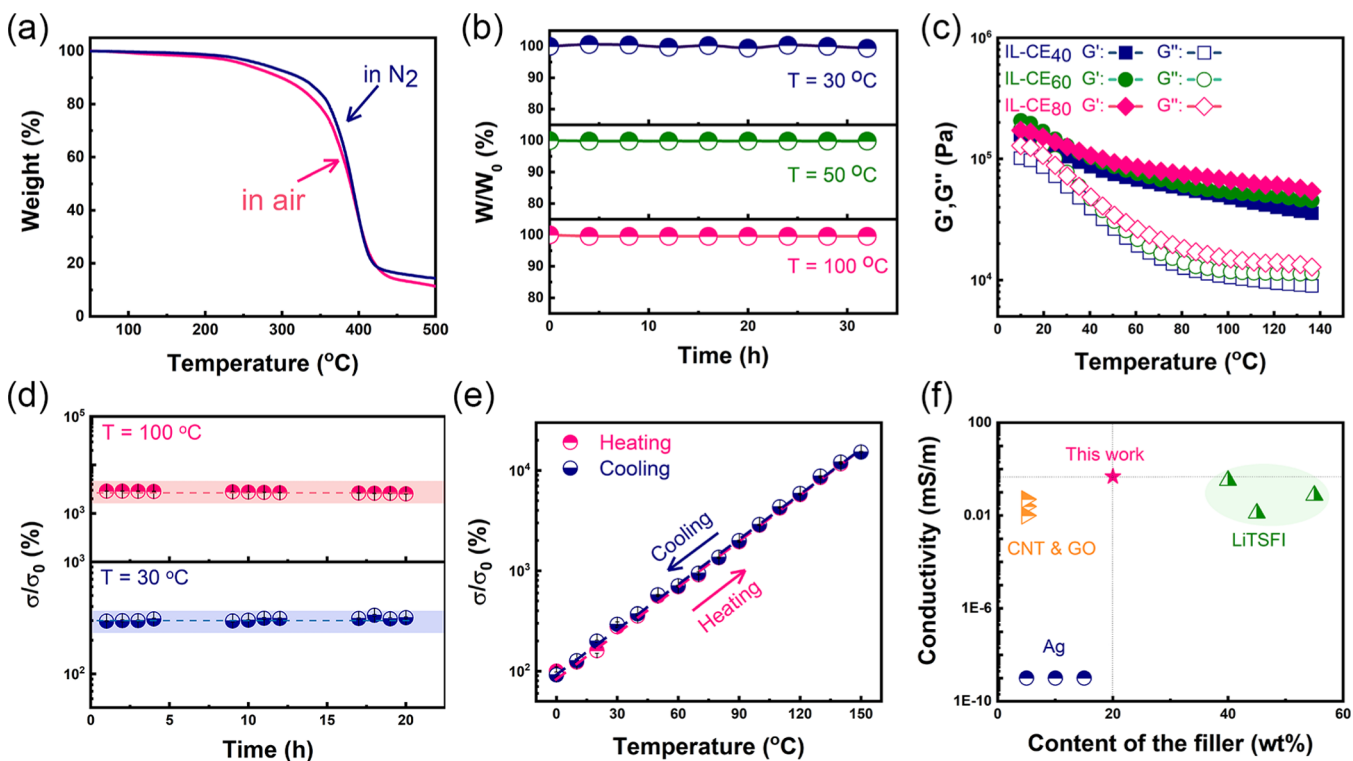


Figure 2. (a) Thermogravimetric curve of the conductive elastomer. (b) Environmental stability testing of the conductive elastomer in open air at test temperatures of 30, 50, and 100 °C. (c) Temperature dependence of G' and G'' for the conductive elastomer from 5 to 140 °C. (d) Stability of the ionic conductivity at room or high temperatures for a long period. (e) Relative changes in ionic conductivity in the temperature range of 0–150 °C. (f) Summary of the conductivity of different conductive elastomers.

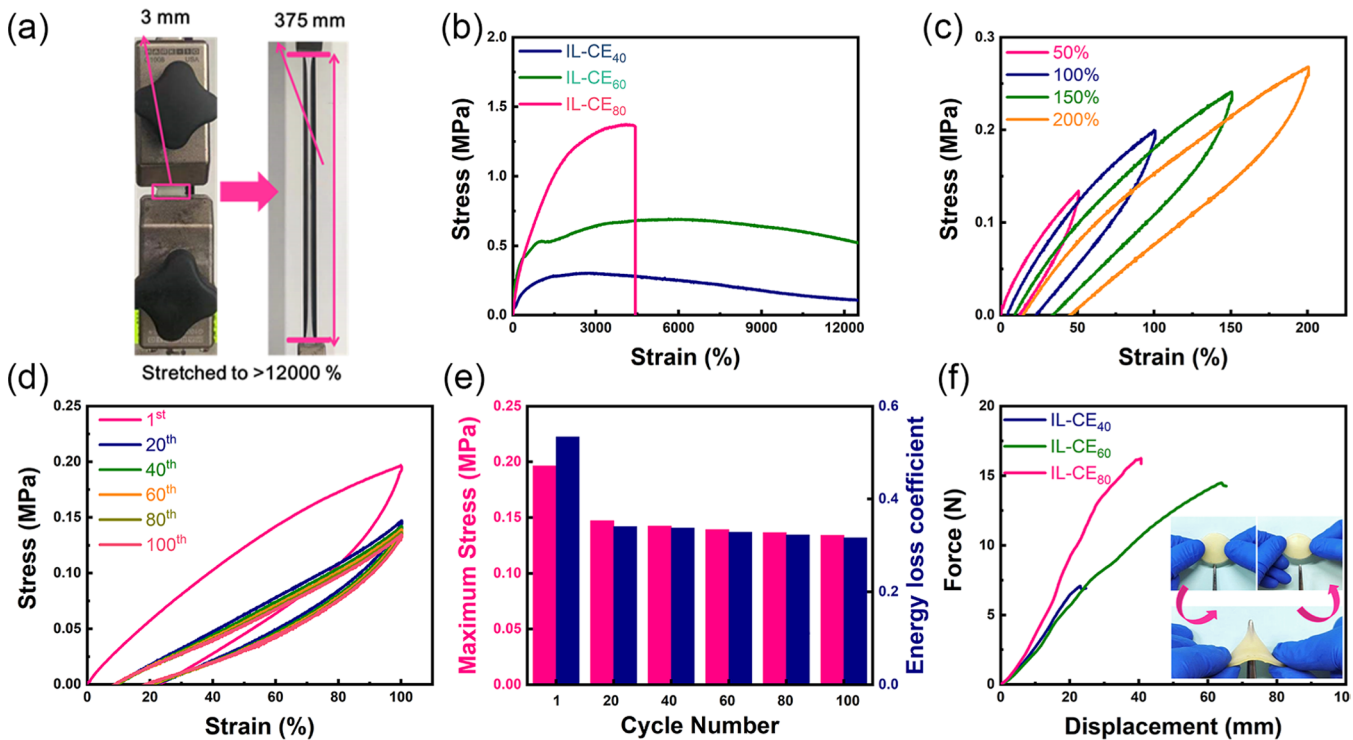


Figure 3. (a) Photographs of the conductive elastomer film before and upon stretching. (b) Stress–strain curves of the conductive elastomer films prepared with different concentrations. (c) Sequential cyclic tensile curves of IL-CE₈₀ at different strains without waiting time between two consecutive loadings. (d) One hundred loading–unloading tensile curves of IL-CE₈₀ at the strain of 100%. (e) Maximum stress and the energy loss coefficient of IL-CE₈₀ during the 100 cycling loading–unloading tests. (f) Force–displacement curves of the different elastomers, measured from the puncture resistance tests. The inset shows the photographs that show the puncture resistance of the conductive elastomer.

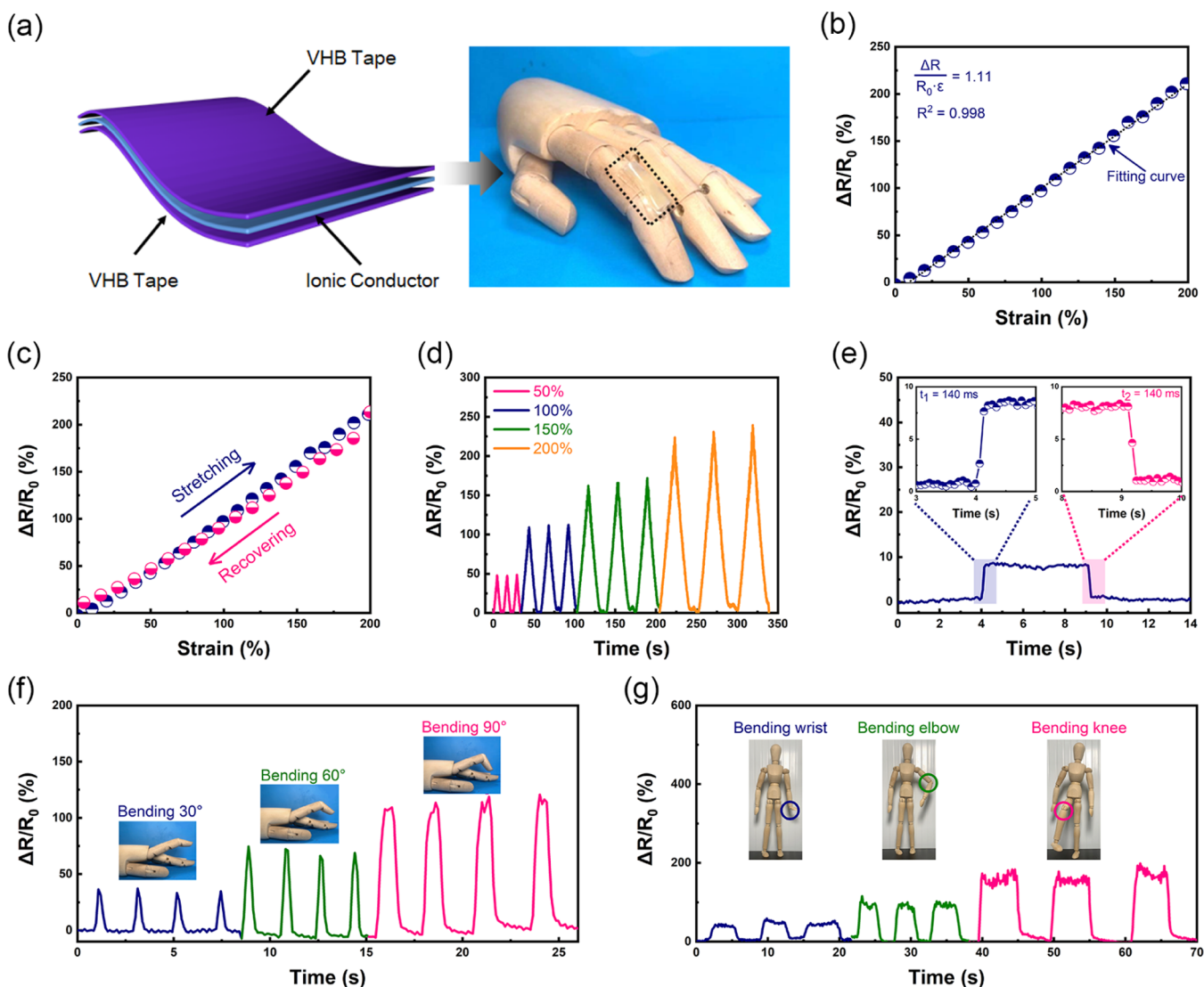


Figure 4. (a) Schematic illustration and the photograph of the IL conductive elastomer-based resistance sensor attached to the puppet's finger. (b) Resistance–strain curve of the sensor in the range of 0–200%. (c) Resistance–strain curves for loading and unloading of strain at 200%. (d) Resistance–strain curves at different strains. (e) Response time of the sensor. The resistance change of the device during the (f) bending of the finger at different angles and (g) the movements of the wrist, elbow, and knee. All of the human motions were simulated by the puppet.

vinyl-SiO₂ from 40 to 80 mg/mL, no remarkable variations in the average droplet size were observed at the beginning. However, after 30 min, only the droplet size of the emulsion with the particle emulsifier concentration of 80 mg/mL did not change obviously, suggesting that the resultant emulsion possessed relatively good stability.

The as-prepared Pickering emulsions were polymerized to afford the IL-based conductive elastomers PnBA/SiO₂/PAA-ILs, which combine the good mechanical properties of elastomers with the high conductivity of ILs. As shown in Figure S3, the characteristic signals belonging to the double bonds of *n*-BA and AA monomers were not observed, indicating that polymerization was complete. Figure S4 shows the SEM morphologies of the resulting elastomer, from which it could be observed that the islandlike PAA-IL microgels were well dispersed in the matrix. Due to this unique structure, the obtained IL-based conductive elastomers possessed many special characteristics. As shown in the thermogravimetric curve (Figure 2a), they possess a high decomposition temperature (up to 225 °C in air and 230 °C in

N₂), indicating that they can be used even under a high temperature. The elastomer's stability at different constant temperatures (30, 50, and 100 °C) in open air was investigated. Figure 2b shows that the weight of the as-prepared elastomer remained unchanged even after 30 h, implying that the elastomer is suitable for applications in open air and a wide range of temperatures. Meanwhile, the effect of humid conditions on the properties of the prepared conductive elastomer was further investigated, as shown in Figure S5. It can be seen that the weight and the conductivity of the elastomers remained almost unchanged within 30 h, implying that the materials possess good stability under different humidities. Temperature sweep measurements for the prepared IL-based elastomers with different contents of vinyl-SiO₂ are shown in Figure 2c. Through the whole testing temperature range (10–140 °C), the elastomer samples retained their solidlike behavior as the storage modulus (*G'*) always remained higher than the loss modulus (*G''*). Besides, the elastomers possessed stable conductivity, confirmed by the material's relative conductivity (σ/σ_0) remaining nearly

constant at a low or high temperature for a long period (Figure 2d). Meanwhile, the conductivity exhibited a temperature-dependent behavior and there was an almost linear relationship between them (Figure 2e). The conductivity of the elastomers was improved with increasing temperature and vice versa. This phenomenon is widely observed in ionic conductors. In Figure 2f, we also compared the IL-based elastomer's conductivity in this work to those reported previously, which are based on carbon materials,^{40–42} silver nanowires,⁴³ and lithium bis-(trifluoromethane sulfonimide).^{44,45} The IL-based elastomer in this work outperforms the former two kinds and is comparable with the last.

Given the inherent features of the PnBA matrix and the cross-linked structure, the obtained IL-based conductive elastomers are expected to exhibit good mechanical properties.⁴⁶ As shown in Figure S6, no trace of polymers was observed, further confirming the cross-linked structure of the as-prepared elastomers. Figure 3a,b shows that the resulting IL-based conductive elastomers possessed a very high stretchability and good mechanical strength. Especially, the elastomers IL-CE₄₀ and IL-CE₆₀ could be surprisingly stretched to about 125 times their original length without rupture, which is better than most of the reported conductive elastomers. In addition, their tensile properties were obviously affected by the contents of vinyl-SiO₂ (Figure 3b). As the contents of vinyl-SiO₂ increased to 80 mg/mL, the fracture stress of the elastomer was up to about 1.46 MPa with the break strain maintained at ca. 5000%. Furthermore, the relationship between the loading rate and the mechanical properties was investigated. From Figure S7, it was observed that the elastomer's mechanical strength obviously increased with the increase of the loading rate from 0.08 to 0.33 s⁻¹, implying that the loading rate significantly affects the mechanical properties of the materials. Apart from excellent mechanical properties, the resulting elastomers also possessed good elasticity. To evaluate the elasticity of the materials, cyclic stress–strain tests without waiting time between two consecutive loadings were first performed with gradually increasing strains. As shown in Figure 3c, the elastomer IL-CE₈₀ could almost recover to its original state after the first tensile cycle with a strain of 50%, and the better elasticity is probably due to the deformation of the micro-ionicgels PAA-ILs during the stretching process. After sequential cycles with larger strains, the elastomer showed observable residual strain, which might be attributed to the partial breakage of the covalent bonds at the interface of the PnBA matrix and micro-ionicgels PAA-ILs. Meanwhile, the pronounced hysteresis at all strains indicated successful energy dissipation during the stretching/releasing process. To characterize the cyclic stability of the elastomers, the uninterrupted cyclic tensile test with a strain of 100% was performed. As shown in Figure 3d, the obvious hysteresis loop could be observed in the first cycle, implying the significant energy dissipation. In the next few cycles, IL-CE₈₀ exhibited excellent fatigue durability, in which the stress–strain curves were almost overlapped. Notably, the maximum stress and the energy loss coefficient were maintained at 68.3 and 59.3%, respectively, without a sustained and noticeable decrease (Figure 3e).^{47,48} To further demonstrate the excellent toughness of the elastomers, puncture resistance tests were performed by puncturing the samples with a needle (inset of Figure 3f).⁴⁹ Figure 3f shows the force–displacement curves of the elastomers with diverse vinyl-SiO₂ nanoparticle contents, from which an obvious increase of force

was observed on increasing the vinyl-SiO₂ nanoparticle contents. The puncture resistance tests were conducted on a universal testing machine by using the puncture resistance testing machine (Figure S8).

With the excellent mechanical properties, good conductivity, and high stability in open air, the fabricated IL-based elastomers can be employed as electrodes for future flexible sensor applications. Figure 4a illustrates the triple-layer structure of the sensor, in which the conductive elastomer was sandwiched between two pieces of VHB.⁵⁰ The fabricated sensor could respond to mechanical stimuli including stretching and bending by electronic signals. Figure 4b shows the relative resistance change ($\Delta R/R_0$) with regard to applied tensile strains up to 200%. The GF value reached 1.11 in this strain range, indicating that the IL-based sensor possessed a high strain sensitivity. Meanwhile, as shown in Figure 4c, there is a reversible linear relationship between strain and resistance with highly stable sensitivity. As the IL-based sensor is subjected to various strains at a fixed strain speed, the relative resistance changes gradually increased with the strain increasing from 50 to 200%, and no obvious shift of the electric signal baseline was observed during the stretching, further confirming the good conductive stability of the sensors (Figure 4d). Moreover, depending on the remarkable conductivity, the response and recovery time of the sensor for the loading and unloading process were both only 120 ms under 10% strain (Figure 4e). The high sensing performance endows the constructed sensors with the capability to accurately monitor various motions of the human body by the changes in the resistance. Figure 4f shows that as the prosthetic finger bends at different angles (30, 60, and 90°), the resistance of the sensor correspondingly changes and the amplitudes of the signals increase with the increasing bending angle. Besides, other body movements, such as elbow, wrist, and knee bending, could also be detected sensitively, as shown in Figure 4g.

4. CONCLUSIONS

In summary, novel conductive elastomers PnBA/SiO₂/PAA-ILs with micro-ionicgels acting as conductive fillers were successfully fabricated via one-pot oil-in-oil Pickering emulsion polymerization, in which the islandlike micro-ionicgels dispersed in the elastic matrix. On the one hand, this strategy makes it realize to integrate the polar ILs into the nonpolar matrix to fabricate conductive elastomers. Most importantly, the resulting IL-based conductive elastomers exhibited a combination of many desirable properties including stability in open air, no leakage of ILs during deformation, a wide operating temperature range, excellent conductivity, large stretchability, good elasticity, and toughness. These properties make the as-prepared nanocomposite elastomers ideal candidates for wearable strain sensors. Thus, we demonstrated the applications of the constructed sensors for accurately monitoring various motions of the human body including finger, elbow, wrist, and knee bending. Overall, this study develops a facile and meaningful approach to fabricate IL-based conductive sensors for human healthcare monitoring.

■ ASSOCIATED CONTENT

Supporting Information

The Supporting Information is available free of charge at <https://pubs.acs.org/doi/10.1021/acsami.1c16061>.

Mechanical measurements, sensing performance, and human detection; synthesis of surface-modified vinyl-SiO₂ (Scheme S1); FT-IR spectra, TGA curve of the modified silica; ¹H NMR of the resulting elastomer; SEM images of the resulting elastomer samples; stability of the material at different humidities; GPC trace of the conductive elastomer; tensile curves at different strain rates; and schematic illustration of the puncture resistance testing machine (Figures S1–S8) (PDF)

AUTHOR INFORMATION

Corresponding Authors

Xiaoshan Fan – State Key Laboratory for Modification of Chemical Fibers and Polymer Materials, College of Materials Science and Engineering, Innovation Center for Textile Science and Technology, Donghua University, Shanghai 201620, P. R. China; orcid.org/0000-0002-0617-7400; Email: xsfan@dhu.edu.cn

Tianxi Liu – State Key Laboratory for Modification of Chemical Fibers and Polymer Materials, College of Materials Science and Engineering, Innovation Center for Textile Science and Technology, Donghua University, Shanghai 201620, P. R. China; Key Laboratory of Synthetic and Biological Colloids, Ministry of Education, School of Chemical and Material Engineering, Jiangnan University, Wuxi 214122, P. R. China; orcid.org/0000-0002-5592-7386; Email: txliu@fudan.edu.cn

Authors

Xiaohui Yu – State Key Laboratory for Modification of Chemical Fibers and Polymer Materials, College of Materials Science and Engineering, Innovation Center for Textile Science and Technology, Donghua University, Shanghai 201620, P. R. China

Yufei Wang – State Key Laboratory for Modification of Chemical Fibers and Polymer Materials, College of Materials Science and Engineering, Innovation Center for Textile Science and Technology, Donghua University, Shanghai 201620, P. R. China

Haopeng Zhang – State Key Laboratory for Modification of Chemical Fibers and Polymer Materials, College of Materials Science and Engineering, Innovation Center for Textile Science and Technology, Donghua University, Shanghai 201620, P. R. China

Complete contact information is available at: <https://pubs.acs.org/10.1021/acsami.1c16061>

Author Contributions

The manuscript was written through the contributions of all authors. All authors have given approval to the final version of the manuscript.

Notes

The authors declare no competing financial interest.

ACKNOWLEDGMENTS

The authors are grateful for the financial support from the National Natural Science Foundation of China (51773035), the Shanghai Rising-Star Program (18QA1400200), and the Shanghai Scientific and Technological Innovation Project (18JC1410600).

REFERENCES

- (1) Wang, J.; Lin, M.-F.; Park, S.; Lee, P. S. Deformable Conductors for Human–Machine Interface. *Mater. Today* **2018**, *21*, 508–526.
- (2) Cao, Y.; Tan, Y. J.; Li, S.; Lee, W. W.; Guo, H.; Cai, Y.; Wang, C.; Tee, B. C. K. Self-healing Electronic Skins for Aquatic Environments. *Nat. Electron.* **2019**, *2*, 75–82.
- (3) Takamatsu, S.; Lonjaret, T.; Ismailova, E.; Masuda, A.; Itoh, T.; Malliaras, G. G. Wearable Keyboard Using Conducting Polymer Electrodes on Textiles. *Adv. Mater.* **2016**, *28*, 4485–4488.
- (4) Hu, B.; Owh, C.; Chee, P. L.; Leow, W. R.; Liu, X.; Wu, Y.-L.; Guo, P.; Loh, X. J.; Chen, X. Supramolecular Hydrogels for Antimicrobial Therapy. *Chem. Soc. Rev.* **2018**, *47*, 6917–6929.
- (5) Cai, Y.; Shen, J.; Yang, C.-W.; Wan, Y.; Tang, H.-L.; Aljarb, A. A.; Chen, C.; Fu, J.-H.; Wei, X.; Huang, K.-W.; Han, Y.; Jonas, S. J.; Dong, X.; Tung, V. Mixed-Dimensional MXene-Hydrogel Heterostructures for Electronic Skin Sensors with Ultrabroad Working Range. *Sci. Adv.* **2020**, *6*, No. eabb5367.
- (6) Wang, Y.; Liu, Y.; Plamthottam, R.; Tebyetekerwa, M.; Xu, J.; Zhu, J.; Zhang, C.; Liu, T. Highly Stretchable and Reconfigurable Ionogels with Unprecedented Thermoplasticity and Ultrafast Self-Healability Enabled by Gradient-Responsive Networks. *Macromolecules* **2021**, *54*, 3832–3844.
- (7) Lei, Z.; Wu, P. A Highly Transparent and Ultra-Stretchable Conductor with Stable Conductivity During Large Deformation. *Nat. Commun.* **2019**, *10*, No. 3429.
- (8) Cai, G.; Wang, J.; Qian, K.; Chen, J.; Li, S.; Lee, P. S. Extremely Stretchable Strain Sensors Based on Conductive Self-Healing Dynamic Cross-Links Hydrogels for Human-Motion Detection. *Adv. Sci.* **2017**, *4*, No. 1600190.
- (9) Liu, X.; Lu, C.; Wu, X.; Zhang, X. Self-Healing Strain Sensors Based on Nanostructured Supramolecular Conductive Elastomers. *J. Mater. Chem. C* **2017**, *5*, 9824–9832.
- (10) Roh, E.; Hwang, B.-U.; Kim, D.; Kim, B.-Y.; Lee, N.-E. Stretchable, Transparent, Ultrasensitive, and Patchable Strain Sensor for Human–Machine Interfaces Comprising a Nanohybrid of Carbon Nanotubes and Conductive Elastomers. *ACS Nano* **2015**, *9*, 6252–6261.
- (11) Duan, L.; Lai, J.-C.; Li, C.-H.; Zuo, J.-L. A Dielectric Elastomer Actuator That Can Self-Heal Integrally. *ACS Appl. Mater. Interfaces* **2020**, *12*, 44137–44146.
- (12) Costa, P.; Oliveira, J.; Horta-Romaris, L.; Abad, M.-J.; Moreira, J. A.; Zapiain, I.; Aguado, M.; Galván, S.; Lanceros-Mendez, S. Piezoresistive Polymer Blends for Electromechanical Sensor Applications. *Compos. Sci. Technol.* **2018**, *168*, 353–362.
- (13) Cao, Z.; Liu, H.; Jiang, L. Transparent, Mechanically Robust, and Ultrastable Ionogels Enabled by Hydrogen Bonding between Elastomers and Ionic Liquids. *Mater. Horiz.* **2020**, *7*, 912–918.
- (14) Catenacci, M. J.; Reyes, C.; Cruz, M. A.; Wiley, B. J. Stretchable Conductive Composites from Cu–Ag Nanowire Felt. *ACS Nano* **2018**, *12*, 3689–3698.
- (15) Choi, S.; Han, S. I.; Kim, D.; Hyeon, T.; Kim, D.-H. High-performance Stretchable Conductive Nanocomposites: Materials, Processes, and Device Applications. *Chem. Soc. Rev.* **2019**, *48*, 1566–1595.
- (16) Zhan, Y.; Oliviero, M.; Wang, J.; Sorrentino, A.; Buonocore, G. G.; Sorrentino, L.; Lavorgna, M.; Xia, H.; Iannace, S. Enhancing the EMI Shielding of Natural Rubber-based Supercritical CO₂ Foams by Exploiting Their Porous Morphology and CNT Segregated Networks. *Nanoscale* **2019**, *11*, 1011–1020.
- (17) Kumar, V.; Lee, G.; Monika; Choi, J.; Lee, D.-J. Studies on Composites Based on HTV and RTV Silicone Rubber and Carbon Nanotubes for Sensors and Actuators. *Polymer* **2020**, *190*, No. 122221.
- (18) Xun, X.; Zhang, Z.; Zhao, X.; Zhao, B.; Gao, F.; Kang, Z.; Liao, Q.; Zhang, Y. Highly Robust and Self-Powered Electronic Skin Based on Tough Conductive Self-Healing Elastomer. *ACS Nano* **2020**, *14*, 9066–9072.
- (19) Natarajan, T. S.; Eshwaran, S. B.; Stöckelhuber, K. W.; Wießner, S.; Pötschke, P.; Heinrich, G.; Das, A. Strong Strain Sensing

Performance of Natural Rubber Nanocomposites. *ACS Appl. Mater. Interfaces* **2017**, *9*, 4860–4872.

(20) Oh, Y.; Yoon, I. S.; Lee, C.; Kim, S. H.; Ju, B.-K.; Hong, J.-M. Selective Photonic Sintering of Ag Flakes Embedded in Silicone Elastomers to Fabricate Stretchable Conductors. *J. Mater. Chem. C* **2017**, *5*, 11733–11740.

(21) Zhao, L.; Yin, Y.; Jiang, B.; Guo, Z.; Qu, C.; Huang, Y. Fast Room-Temperature Self-Healing Siloxane Elastomer for Healable Stretchable Electronics. *J. Colloid Interface Sci.* **2020**, *573*, 105–114.

(22) Park, J.; Kim, G.; Lee, B.; Lee, S.; Won, P.; Yoon, H.; Cho, H.; Ko, S. H.; Hong, Y. Highly Customizable Transparent Silver Nanowire Patterning via Inkjet-Printed Conductive Polymer Templates Formed on Various Surfaces. *Adv. Mater. Technol.* **2020**, *5*, No. 2000042.

(23) Qian, W.; Texter, J.; Yan, F. Frontiers in Poly(ionic liquid)s: Syntheses and Applications. *Chem. Soc. Rev.* **2017**, *46*, 1124–1159.

(24) MacFarlane, D. R.; Forsyth, M.; Howlett, P. C.; Kar, M.; Passerini, S.; Pringle, J. M.; Ohno, H.; Watanabe, M.; Yan, F.; Zheng, W.; Zhang, S.; Zhang, J. Ionic Liquids and Their Solid-State Analogues as Materials for Energy Generation and Storage. *Nat. Rev. Mater.* **2016**, *1*, 1–15.

(25) Wang, Y.; Sun, S.; Wu, P. Adaptive Ionogel Paint from Room-Temperature Autonomous Polymerization of α -Thioctic Acid for Stretchable and Healable Electronics. *Adv. Funct. Mater.* **2021**, *31*, No. 2101494.

(26) Park, D. H.; Park, H. W.; Chung, J. W.; Nam, K.; Choi, S.; Chung, Y. S.; Hwang, H.; Kim, B.; Kim, D. H. Highly Stretchable, High-Mobility, Free-Standing All-Organic Transistors Modulated by Solid-State Elastomer Electrolytes. *Adv. Funct. Mater.* **2019**, *29*, No. 1808909.

(27) Ren, Y.; Liu, Z.; Jin, G.; Yang, M.; Shao, Y.; Li, W.; Wu, Y.; Liu, L.; Yan, F. Electric-Field-Induced Gradient Ionogels for Highly Sensitive, Broad-Range-Response, and Freeze/Heat-Resistant Ionic Fingers. *Adv. Mater.* **2021**, *33*, No. 2008486.

(28) Zhang, B.; Zhang, X.; Wan, K.; Zhu, J.; Xu, J.; Zhang, C.; Liu, T. Dense Hydrogen-Bonding Network Boosts Ionic Conductive Hydrogels with Extremely High Toughness, Rapid Self-Recovery, and Autonomous Adhesion for Human-Motion Detection. *Research* **2021**, *2021*, No. 9761625.

(29) Li, M.; Liu, B.; Fan, X.; Liu, X.; Liu, J.; Ding, J.; Han, X.; Deng, Y.; Hu, W.; Zhong, C. Long-Shelf-Life Polymer Electrolyte Based on Tetraethylammonium Hydroxide for Flexible Zinc–Air Batteries. *ACS Appl. Mater. Interfaces* **2019**, *11*, 28909–28917.

(30) Yu, J.; Liu, S.; Duan, G.; Fang, H.; Hou, H. Dense and Thin Coating of Gel Polymer Electrolyte on Sulfur Cathode toward High Performance Li-sulfur Battery. *Compos. Commun.* **2020**, *19*, 239–245.

(31) Jiang, N.; Li, H.; Hu, D.; Xu, Y.; Hu, Y.; Zhu, Y.; Han, X.; Zhao, G.; Chen, J.; Chang, X.; Xi, M.; Yuan, Q. Stretchable Strain and Temperature Sensor based on Fibrous Polyurethane Film Saturated with Ionic Liquid. *Compos. Commun.* **2021**, *27*, No. 100845.

(32) Okafuji, A.; Kohno, Y.; Nakamura, N.; Ohno, H. Design of Thermoresponsive Poly(ionic liquid) Gels Containing Proline Units to Catalyze Aldol Reaction in Water. *Polymer* **2018**, *134*, 20–23.

(33) Liang, L.; Yuan, W.; Chen, X.; Liao, H. Flexible, Nonflammable, Highly Conductive and High-Safety Double Cross-Linked Poly(ionic liquid) as Quasi-solid Electrolyte for High Performance Lithium-ion Batteries. *Chem. Eng. J.* **2021**, *421*, No. 130000.

(34) Gao, N.; He, Y.; Tao, X.; Xu, X.-Q.; Wu, X.; Wang, Y. Crystal-confined Freestanding Ionic Liquids for Reconfigurable and Repairable Electronics. *Nat. Commun.* **2019**, *10*, No. 547.

(35) Sun, J.; Yuan, Y.; Lu, G.; Li, L.; Zhu, X.; Nie, J. A Transparent, Stretchable, Stable, Self-adhesive Ionogel-based Strain Sensor for Human Motion Monitoring. *J. Mater. Chem. C* **2019**, *7*, 11244–11250.

(36) Liu, X.; Yu, L.; Zhu, Z.; Nie, Y.; Skov, A. L. Silicone-Ionic Liquid Elastomer Composite with Keratin as Reinforcing Agent Utilized as Pressure Sensor. *Macromol. Rapid Commun.* **2021**, *42*, No. 2000602.

(37) Liu, S.; Fan, X.; He, C. Improving the Fracture Toughness of Epoxy with Nanosilica-Rubber Core-Shell Nanoparticles. *Compos. Sci. Technol.* **2016**, *125*, 132–140.

(38) Mostafa, H. Y.; Hussain, A. I.; El-Masry, A. M.; Maher, A. Novel Core–Shell of Polymethyl Methacrylate/butyl Acrylate/vinyl Silica Nanocomposite Particles through Seed Emulsion Polymerization. *Polym.-Plast. Technol. Eng.* **2017**, *56*, 411–420.

(39) Jia, X.; Li, Y.; Cheng, Q.; Zhang, S.; Zhang, B. Preparation and Properties of Poly(vinyl alcohol)/Silica Nanocomposites Derived from Copolymerization of Vinyl Silica Nanoparticles and Vinyl Acetate. *Eur. Polym. J.* **2007**, *43*, 1123–1131.

(40) Le, H. H.; Abhijeet, S.; Ilisch, S.; Klehm, J.; Henning, S.; Beiner, M.; Sarkawi, S. S.; Dierkes, W.; Das, A.; Fischer, D.; Stöckelhuber, K. W.; Wiessner, S.; Khatiwada, S. P.; Adhikari, R.; Pham, T.; Heinrich, G.; Radosch, H. J. The Role of Linked Phospholipids in the Rubber-filler Interaction in Carbon Nanotube (CNT) Filled Natural Rubber (NR) Composites. *Polymer* **2014**, *55*, 4738–4747.

(41) Wu, H.; Yao, P.; Ning, N.; Zhang, L.; Tian, H.; Wu, Y.; Tian, M. A Novel Dielectric Elastomer by Constructing Dual-network Structure of Carbon Nanotubes and Rubber Nanoparticles in Dynamically Vulcanized Thermoplastic Elastomer. *RSC Adv.* **2016**, *6*, 32932–32939.

(42) Costa, P.; Gonçalves, S.; Mora, H.; Carabineiro, S. A. C.; Viana, J. C.; Lanceros-Mendez, S. Highly Sensitive Piezoresistive Graphene-Based Stretchable Composites for Sensing Applications. *ACS Appl. Mater. Interfaces* **2019**, *11*, 46286–46295.

(43) Liu, C.; Wu, W.; Wang, Y.; Wang, Z.; Chen, Q. Silver-coated Thermoplastic Polyurethane Hybrid Granules for Dual-Functional Elastomer Composites with Exceptional Thermal Conductive and Electromagnetic Interference Shielding Performances. *Compos. Commun.* **2021**, *25*, No. 100719.

(44) Goujon, L. J.; Khaldi, A.; Maziz, A.; Plesse, C.; Nguyen, G. T. M.; Aubert, P.-H.; Vidal, F.; Chevrot, C.; Teyssié, D. Flexible Solid Polymer Electrolytes Based on Nitrile Butadiene Rubber/Poly(ethylene oxide) Interpenetrating Polymer Networks Containing Either LiTFSI or EMITFSI. *Macromolecules* **2011**, *44*, 9683–9691.

(45) Shi, L.; Zhu, T.; Gao, G.; Zhang, X.; Wei, W.; Liu, W.; Ding, S. Highly Stretchable and Transparent Ionic Conducting Elastomers. *Nat. Commun.* **2018**, *9*, No. 2630.

(46) Yamazaki, H.; Takeda, M.; Kohno, Y.; Ando, H.; Urayama, K.; Takigawa, T. Dynamic Viscoelasticity of Poly(butyl acrylate) Elastomers Containing Dangling Chains with Controlled Lengths. *Macromolecules* **2011**, *44*, 8829–8834.

(47) Wang, A.; Wang, Y.; Zhang, B.; Wan, K.; Zhu, J.; Xu, J.; Zhang, C.; Liu, T. Hydrogen-bonded Network Enables Semi-Interpenetrating Ionic Conductive Hydrogels with High Stretchability and Excellent Fatigue Resistance for Capacitive/Resistive Bimodal Sensors. *Chem. Eng. J.* **2021**, *411*, No. 128506.

(48) Xu, Y.; Feng, Q.; Zhang, C.; Liu, T. Wet-spinning of IonicLiquid@Elastomer Coaxial Fibers with High Stretchability and Wide Temperature Resistance for Strain Sensors. *Compos. Commun.* **2021**, *25*, No. 100693.

(49) Li, Z.; Zhu, Y.-L.; Niu, W.; Yang, X.; Jiang, Z.; Lu, Z.-Y.; Liu, X.; Sun, J. Healable and Recyclable Elastomers with Record-High Mechanical Robustness, Unprecedented Crack Tolerance, and Superhigh Elastic Restorability. *Adv. Mater.* **2021**, *33*, No. 2101498.

(50) Zhang, J.; Wan, L.; Gao, Y.; Fang, X.; Lu, T.; Pan, L.; Xuan, F. Highly Stretchable and Self-Healable MXene/Polyvinyl Alcohol Hydrogel Electrode for Wearable Capacitive Electronic Skin. *Adv. Electron. Mater.* **2019**, *5*, No. 1900285.